SPECTRAL-DOMAIN ANALYSIS

Many numerical methods exist for analyzing microwave and millimeter-wave passive structures. Among them, spectral-domain analysis (SDA) is one of the most popular. It was developed by Itoh and Mitra in 1974 (1). In 1978, Itoh also presented an SDA version for quasistatic analysis (2). SDA is basically a Fourier-transformed version of the integral equation method. However, as compared to the conventional space-domain integral equation method, SDA has several advantages. Its formulation results in a system of coupled algebraic equations instead of coupled integral equations. Closed-form expressions can be easily obtained for the Green's functions. In addition, incorporation of physical conditions of analyzed structures via the so-called basis functions is achieved, and the obtained solutions are stationary. These features make SDA numerically simpler and more efficient than the conventional integral equation method. SDA has been used extensively in analyzing planar transmission lines (e.g., Ref. 3). In this article, we present a detailed formulation of SDA for planar transmission lines in both quasistatic and dynamic domains. Other applications of SDA, to resonators and antenna and scattering problems, can be found in Refs. 4, 5, and 6, respectively.

FORMULATION OF THE SPECTRAL DOMAIN ANALYSIS

Figure 1 shows a cross section of the multilayer coplanar waveguide (CPW) to be analyzed. The central and ground strips are assumed to be perfect electric conductors of zero thickness, uniform and infinite in the z direction. The formulation for the case of finite strip thickness is discussed in Ref. 7. The dielectric substrates are assumed to be lossless. The enclosure or channel is assumed to be a perfect electrical conductor and is used to simplify some of the analysis and computation, but the resulting analysis can be used for an open structure by letting the appropriate dimensions be large. The eigenmodes existing in the considered structure consist of both TE and TM fields. Although SDA can produce results for all of the real and complex eigenmodes for this structure (8), in this article we are restricted to the analysis of the real eigenmodes, including the dominant (CPW) mode, for the purpose of illustrating SDA. Due to the effect of multiple dielectrics surrounding the metallic strips, the dominant CPW mode is quasi TEM.

Quasistatic Spectral-Domain Analysis

A quasistatic analysis solves the two-dimensional Laplace's equation for the electric potential in the transverse plane subject to appropriate boundary conditions in the space domain,

$$\frac{\partial^2\phi_i(x, y)}{\partial x^2} + \frac{\partial^2\phi_i(x, y)}{\partial y^2} = 0, \qquad i = 1, 2, 3 \tag{1}$$

where $\phi_i(x, y)$ is the unknown potential in the ith region. The quasistatic SDA, on the other hand, solves Laplace's equation by applying a moment method, Galerkin's technique, in the Fourier transform, or spectral, domain (2). The analysis obtains the charge density on the central strip, and from this the per-unit-length (PUL) capacitance is obtained. The PUL capacitance can then be used to determine the effective dielectric constant and characteristic impedance of the transmission line. The boundary conditions are derived from the fact that $\phi(x, y)$ is continuous everywhere and $\hat{\boldsymbol{n}} \cdot (\boldsymbol{D}_2 - \boldsymbol{D}_1) = \rho_s$ at the upper interface (between the first and second layers), where $\boldsymbol{D}_i$, $i = 1, 2$, is the electric flux density in region i, $\hat{\boldsymbol{n}}$ is the unit vector normal to the interface, and ρ_s is the surface charge density. The boundary conditions are

$$\phi_i(0, y) = \phi_i(a, y) = 0 \tag{2}$$

$$\phi_1(x, b) = \phi_3(x, 0) = 0 \tag{3}$$

$$\phi_1(x, h_2 + h_3) = \phi_2(x, h_2 + h_3) = V^{\mathrm{U}}(x) \tag{4}$$

$$\phi_2(x, h_3) = \phi_3(x, h_3) \tag{5}$$

$$\epsilon_{r2}\frac{\partial\phi_2}{\partial y}\bigg|_{y=h_2+h_3} - \epsilon_{r1}\frac{\partial\phi_1}{\partial y}\bigg|_{y=h_2+h_3} = \frac{\rho_s(x)}{\epsilon_0} \tag{6}$$

$$\epsilon_{r3}\frac{\partial\phi_3}{\partial y}\bigg|_{y=h_3} - \epsilon_{r2}\frac{\partial\phi_2}{\partial y}\bigg|_{y=h_3} = 0 \tag{7}$$

where ϵ_0 is the free-space permittivity and ϵ_{ri}, $i = 1, 2, 3$, is the relative dielectric constant of the ith layer; $V^{\mathrm{U}}(x)$ denotes the potential at the upper interface and can be expressed as

$$V^{\mathrm{U}}(x) = V_0(x) + V(x) \tag{8}$$

$V_0(x) = V_0$ on the central strip and zero elsewhere; we choose the value of V_0. The ground strips are assumed to be at zero potential. $V(x)$ is the unknown potential on the two slots and zero on the central and ground strips. The surface charge density, ρ_s, can be described as

$$\rho_s(x) = \rho_{s1}(x) + \rho_{s2}(x) + \rho_{s3}(x) \tag{9}$$

where $\rho_{s1}(x)$, $\rho_{s2}(x)$, and $\rho_{s3}(x)$ are unknown charge densities on the central, left, and right ground strips, respectively, and are nonzero only on the corresponding strips.

The Fourier transform used is defined as follows:

$$\tilde{f}(\alpha_n, y) = \frac{2}{a}\int_0^a f(x, y)\sin\alpha_n x\, dx \tag{10}$$

where $\alpha_n = n\pi/a$, $n = 1, 2, 3, \ldots$ denoting the spectral order or term. This choice for the Fourier transform variable α_n will cause the boundary conditions of Eq. (2) on $\phi_i(x, y)$ to be met automatically.

Transforming Eqs. (1) to (9) gives

$$\frac{\partial^2\tilde{\phi}_i}{\partial y^2} - \alpha_n^2\tilde{\phi}_i = 0 \tag{11}$$

$$\tilde{\phi}_1(\alpha_n, b) = \tilde{\phi}_3(\alpha_n, 0) = 0 \tag{12}$$

$$\tilde{\phi}_1(\alpha_n, h_2 + h_3) = \tilde{\phi}_2(\alpha_n, h_2 + h_3) = \tilde{V}^{\mathrm{U}}(\alpha_n) \tag{13}$$

$$\tilde{\phi}_2(\alpha_n, h_3) = \tilde{\phi}_3(\alpha_n, h_3) \tag{14}$$

$$\epsilon_{r2}\frac{\partial\tilde{\phi}_2}{\partial y}\bigg|_{y=h_2+h_3} - \epsilon_{r1}\frac{\partial\tilde{\phi}_1}{\partial y}\bigg|_{y=h_2+h_3} = \frac{\tilde{\rho}_s(\alpha_n)}{\epsilon_0} \tag{15}$$

$$\epsilon_{r3}\frac{\partial\tilde{\phi}_3}{\partial y}\bigg|_{y=h_3} - \epsilon_{r2}\frac{\partial\tilde{\phi}_2}{\partial y}\bigg|_{y=h_3} = 0 \tag{16}$$

$$\tilde{V}^{\mathrm{U}}(\alpha_n) = \tilde{V}_0(\alpha_n) + \tilde{V}(\alpha_n) \tag{17}$$

$$\tilde{\rho}_s(\alpha_n) = \tilde{\rho}_{s1}(\alpha_n) + \tilde{\rho}_{s2}(\alpha_n) + \tilde{\rho}_{s3}(\alpha_n) \tag{18}$$

The solution of Eq. (11) is well known. A judicious choice yields the following forms, which satisfy Eq. (12):

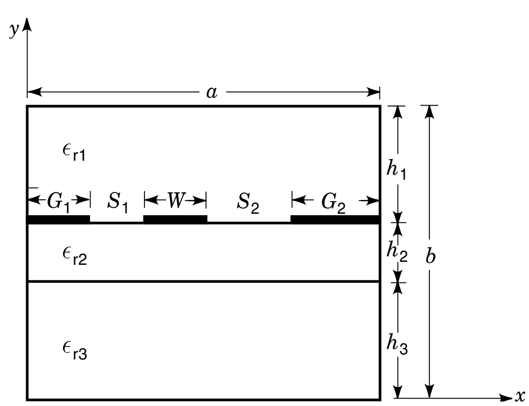

Figure 1. A cross section of the coplanar waveguide used for illustrating SDA.

$$\tilde{\phi}_1(\alpha_n, y) = A \sinh \alpha_n (b - y) \tag{19}$$

$$\tilde{\phi}_2(\alpha_n, y) = B \sinh \alpha_n (y - h_3) + C \cosh \alpha_n (y - h_3) \tag{20}$$

$$\tilde{\phi}_3(\alpha_n, y) = D \sinh \alpha_n y \tag{21}$$

where A, B, C, and D are unknown functions of α_n. Substituting Eqs. (19) to (21) into Eqs. (13)to (16) and solving for $\tilde{V}^{\mathrm{U}}(\alpha_n)$ in terms of $\tilde{\rho}_{\mathrm{s}}(\alpha_n)$ yields

$$\tilde{G}(\alpha_n)\tilde{\rho}_{\mathrm{s}}(\alpha_n) = \tilde{V}^{\mathrm{U}}(\alpha_n) \tag{22}$$

where $\tilde{G}(\alpha_n)$ is the spectral-domain Green's function given as

$$\begin{aligned}\tilde{G}(\alpha_n) = {}& \tanh \alpha_n h_1 \left(\frac{\epsilon_{\mathrm{r3}}}{\epsilon_{\mathrm{r2}}} \tanh \alpha_n h_2 + \tanh \alpha_n h_3\right) \\ & \times \left\{\epsilon_0 \alpha_n \tanh \alpha_n h_2 \left[\epsilon_{\mathrm{r3}} \left(\frac{\epsilon_{\mathrm{r1}}}{\epsilon_{\mathrm{r2}}} + \tanh \alpha_n h_1 \coth \alpha_n h_2\right)\right.\right. \\ & \left.\left. + \tanh \alpha_n h_3 \,(\epsilon_{\mathrm{r1}} \coth \alpha_n h_2 + \epsilon_{\mathrm{r2}} \tanh \alpha_n h_1)\right]\right\}^{-1}\end{aligned} \tag{23}$$

We now begin to apply the Galerkin's technique in the spectral domain by expressing each strip's charge density as a truncated summation of basis functions in the space domain as

$$\rho_{\mathrm{s}}(x) \approx \sum_{j=1}^{3} \sum_{i=1}^{N_j} d_{ji} \rho_{\mathrm{s}ji}(x) \tag{24}$$

where $\rho_{sji}(x)$ describes the charge distribution on the jth strip and is nonzero only on that strip, d_{ji} is the unknown coefficient, and N_j denotes the number of basis functions used for the jth strip's charge density. In the spectral domain,

$$\tilde{\rho}_{\mathrm{s}}(\alpha_n) \approx \sum_{j=1}^{3} \sum_{i=1}^{N_j} d_{ji} \tilde{\rho}_{\mathrm{s}ji}(\alpha_n) \tag{25}$$

Substitute Eq. (25) into Eq. (22), multiply by $\tilde{\rho}_{sji}(\alpha_n)$ for $j = 1, 2, 3$ and $i = 1, 2, \ldots, N_j$, and sum over α_n. This results in a system of coupled linear algebraic equations

$$\begin{aligned}&\sum_{i=1}^{N_1}\left(\sum_{n=1}^{\infty}\tilde{\rho}_{\mathrm{s}1j}\tilde{G}\tilde{\rho}_{\mathrm{s}1i}\right)d_{1i} + \sum_{i=1}^{N_2}\left(\sum_{n=1}^{\infty}\tilde{\rho}_{\mathrm{s}1j}\tilde{G}\tilde{\rho}_{\mathrm{s}2i}\right)d_{2i} \\ &\quad + \sum_{i=1}^{N_3}\left(\sum_{n=1}^{\infty}\tilde{\rho}_{\mathrm{s}1j}\tilde{G}\tilde{\rho}_{\mathrm{s}3i}\right)d_{3i} = \frac{2}{a}V_0\int_{G_1+S_1}^{G_1+S_1+W}\rho_{\mathrm{s}1j}(x)\,dx, \\ &\qquad j = 1, 2, \ldots, N_1\end{aligned} \tag{26}$$

$$\begin{aligned}&\sum_{i=1}^{N_2}\left(\sum_{n=1}^{\infty}\tilde{\rho}_{\mathrm{s}2j}\tilde{G}\tilde{\rho}_{\mathrm{s}1i}\right)d_{1i} + \sum_{i=1}^{N_2}\left(\sum_{n=1}^{\infty}\tilde{\rho}_{\mathrm{s}2j}\tilde{G}\tilde{\rho}_{\mathrm{s}2i}\right)d_{2i} \\ &\quad + \sum_{i=1}^{N_3}\left(\sum_{n=1}^{\infty}\tilde{\rho}_{\mathrm{s}2j}\tilde{G}\tilde{\rho}_{\mathrm{s}3i}\right)d_{3i} = 0, \qquad j = 1, 2, \ldots, N_2\end{aligned} \tag{27}$$

$$\begin{aligned}&\sum_{i=1}^{N_2}\left(\sum_{n=1}^{\infty}\tilde{\rho}_{\mathrm{s}3j}\tilde{G}\tilde{\rho}_{\mathrm{s}1i}\right)d_{1i} + \sum_{i=1}^{N_2}\left(\sum_{n=1}^{\infty}\tilde{\rho}_{\mathrm{s}3j}\tilde{G}\tilde{\rho}_{\mathrm{s}2i}\right)d_{2i} \\ &\quad + \sum_{i=1}^{N_3}\left(\sum_{n=1}^{\infty}\tilde{\rho}_{\mathrm{s}3j}\tilde{G}\tilde{\rho}_{\mathrm{s}3i}\right)d_{3i} = 0, \qquad j = 1, 2, \ldots, N_3\end{aligned} \tag{28}$$

The use of the Galerkin's technique enables us to eliminate the unknown voltage $\tilde{V}$ by applying Parseval's theorem to the right-hand sides. Specifically, Parseval's theorem eliminates the summations involving $\tilde{V}$, because the charge densities and voltages are nonzero in complementary regions in the space domain. Furthermore, two summations involving known voltages are eliminated. Equations (26) to (28) can be solved for the unknown coefficients of the charge density basis functions. The transmission line's PUL capacitance is given as

$$C = \frac{Q_0}{V_0} = \frac{\displaystyle\sum_{i=1}^{N_1} d_{1i} \int_{G_1+S_1}^{G_1+S_1+W} \rho_{\mathrm{s}1i}(x)\,dx}{V_0} \tag{29}$$

which can then be used to calculate the characteristic impedance and effective dielectric constant as

$$Z_{\mathrm{c}} = \frac{1}{c\sqrt{CC_{\mathrm{a}}}} \tag{30}$$

and

$$\epsilon_{\mathrm{r\,eff}} = \frac{C}{C_{\mathrm{a}}} \tag{31}$$

respectively, where c is the free-space velocity and C_{a} is the capacitance per unit length with the dielectrics removed.

To obtain numerical results, we need to choose basis functions for the charge densities, $\rho_{sji}(x)$, with $j = 1, 2, 3$ for the central strip and left and right ground strips, respectively. These basis functions influence strongly the numerical efficiency of the solution process and the accuracy of the solutions. The computation time can be reduced significantly if the chosen basis functions describe closely the actual behavior of the charge distributions and have closed-form Fourier transforms. In addition, the basis functions should form complete sets, so that the solution accuracy can be enhanced by increasing the number of basis functions. Furthermore, they should be twice continuously differentiable to avoid spurious solutions. The basis functions used for the considered problem have the form

$$\rho_{\mathrm{s}1i}(x) = \frac{\cos\left((i-1)\pi\dfrac{x - S_1 - G_1}{W}\right)}{\sqrt{1 - \left(\dfrac{2(x - S_1 - G_1) - W}{W}\right)^2}} \tag{32}$$

$$\rho_{\mathrm{s}2i}(x) = \frac{\cos\left[\left(i - \frac{1}{2}\right)\pi\dfrac{x - G_1}{G_1}\right]}{\sqrt{1 - (x/G_1)^2}} \tag{33}$$

$$\rho_{\mathrm{s}3i}(x) = \frac{\cos\left(\left(i - \frac{1}{2}\right)\pi\dfrac{x - a + G_2}{G_2}\right)}{\sqrt{1 - \left(\dfrac{a - x}{G_2}\right)^2}} \tag{34}$$

whose Fourier transforms are obtained as

$$\tilde{\rho}_{s1i}(\alpha_n) = \frac{\pi W}{2a}\left\{J_0\left(\left|\frac{(i-1)\pi + \alpha_n W}{2}\right|\right) \sin \left[\frac{(i-1)\pi}{2} + \alpha_n\left(S_1 + G_1 + \frac{W}{2}\right)\right] - J_0\left(\left|\frac{(i-1)\pi - \alpha_n W}{2}\right|\right) \sin \left[\frac{(i-1)\pi}{2} - \alpha_n\left(S_1 + G_1 + \frac{W}{2}\right)\right]\right\} \quad (35)$$

$$\tilde{\rho}_{s2i}(\alpha_n) = (-1)^i \frac{\pi G_1}{2a}\left\{J_0\left(\left|(i-\tfrac{1}{2})\pi + \alpha_n G_1\right|\right) - J_0\left(\left|(i-\tfrac{1}{2})\pi - \alpha_n G_1\right|\right)\right\} \quad (36)$$

$$\tilde{\rho}_{s3i}(\alpha_n) = (-1)^{i+n+1} \frac{\pi G_2}{2a}\left\{J_0\left(\left|(i-\tfrac{1}{2})\pi + \alpha_n G_2\right|\right) - J_0\left(\left|(i-\tfrac{1}{2})\pi - \alpha_n G_2\right|\right)\right\} \quad (37)$$

where J_0 stands for the zeroth-order Bessel function of the first kind. A remark needs to be made at this point, that the numbers of both basis functions N_j and spectral terms n affect the accuracy of the numerical results. The larger these numbers, the more accurate the results, but at the expense of the computation time. For most engineering purposes, three basis functions and two hundred spectral terms are sufficient.

As a demonstration of the quasistatic SDA, we show in Fig. 2 the calculated values of the characteristic impedance and effective dielectric constant for the CPW versus the right gap.

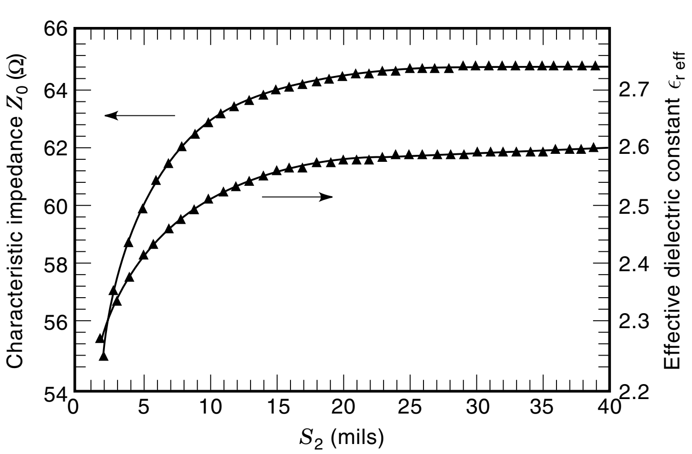

Figure 2. Calculated characteristic impedance and effective dielectric constant of the coplanar waveguide using the quasistatic SDA. a = 100 mil, $W = S_1 = 2G_1$ = 20 mil, $h_1 = h_3 = 4h_2$ = 20 mil, $\epsilon_{r1} = 1$, $\epsilon_{r2} = 2.2$, $\epsilon_{r3} = 10.5$. (1 mil = 0.001 in. = 0.0025 cm.)

Dynamic Spectral-Domain Analysis

The dynamic SDA solves the wave equation in the spectral domain using Galerkin's technique (1). The analysis can obtain the propagation constants, effective dielectric constants, and characteristic impedances of the transmission line for all of the eigenmodes. In essence, its formulation is similar to that for the quasistatic case.

To simplify the analysis without loss of generality, we consider here a symmetrical CPW; i.e., we let $G_1 = G_2 = G$ and $S_1 = S_2 = S$. The SDA for the asymmetrical CPW can be found in Ref. 8. Let $\tilde{\psi}_{ei}(\alpha_n, y)$ and $\tilde{\psi}_{hi}(\alpha_n, y)$ represent the scalar electric and magnetic potentials associated with the TM and TE modes in the ith region in the spectral domain, respectively. The Fourier-transformed Helmholtz equations of these potentials can be expressed as

$$\frac{\partial^2}{\partial y^2}\tilde{\psi}_{pi}(\alpha_n, y) - \gamma_i^2 \tilde{\psi}_{pi}(\alpha_n, y) = 0, \qquad p = e, h, \quad i = 1, 2, 3 \quad (38)$$

where

$$\gamma_i^2 = \beta^2 + \alpha_n^2 - k_i^2 \quad (39)$$

β is the propagation constant, and $k_i = \omega\sqrt{\epsilon_i \mu_i}$ is the wave number in region i. Here ω is the angular frequency, and ϵ_i and μ_i are the permittivity and permeability of medium i, respectively.

The boundary conditions are:

For $0 \le x \le a$, $y = h_3$,

$$E_{x3}(x, h_3) = E_{x2}(x, h_3) \quad (40)$$

$$E_{z3}(x, h_3) = E_{z2}(x, h_3) \quad (41)$$

$$H_{x3}(x, h_3) = H_{x2}(x, h_3) \quad (42)$$

$$H_{z3}(x, h_3) = H_{z2}(x, h_3) \quad (43)$$

For $0 \le x \le a$, $y = h_2 + h_3$,

$$E_{x2}(x, h_2 + h_3) = E_{x1}(x, h_2 + h_3) = E_x(x) \quad (44)$$

$$E_{z2}(x, h_2 + h_3) = E_{z1}(x, h_2 + h_3) = E_z(x) \quad (45)$$

$$H_{x2}(x, h_2 + h_3) - H_{x1}(x, h_2 + h_3) = J_z(x) \quad (46)$$

$$H_{z2}(x, h_2 + h_3) - H_{z1}(x, h_2 + h_3) = -J_x(x) \quad (47)$$

For $0 \le x \le a$, $y = 0$ and b,

$$E_{x3}(x, y) = E_{x1}(x, y) = E_{z3}(x, y) = E_{z1}(x, y) = 0 \quad (48)$$

Here E_i and H_i, i = 1, 2, 3, are the electric and magnetic fields in region i, respectively. $E_x(x)$ and $E_z(x)$ are the x and z components of the unknown electric field on the two slots; they are nonzero on the slots and zero elsewhere. $J_x(x)$ and $J_z(x)$ are the total x- and z-directed current densities on the central and ground strips, and they are nonzero only on those strips. Now taking the Fourier transform of Eqs. (40) to (48) gives

$$\tilde{E}_{x3}(\alpha_n, h_3) = \tilde{E}_{x2}(\alpha_n, h_3) \quad (49)$$

$$\tilde{E}_{z3}(\alpha_n, h_3) = \tilde{E}_{z2}(\alpha_n, h_3) \quad (50)$$

$$\tilde{H}_{x3}(\alpha_n, h_3) = \tilde{H}_{x2}(\alpha_n, h_3) \quad (51)$$

$$\tilde{H}_{z3}(\alpha_n, h_3) = \tilde{H}_{z2}(\alpha_n, h_3) \quad (52)$$

$$\tilde{E}_{x2}(\alpha_n, h_2 + h_3) = \tilde{E}_{x1}(\alpha_n, h_2 + h_3) = \tilde{E}_x(\alpha_n) \quad (53)$$

$$\tilde{E}_{z2}(\alpha_n, h_2 + h_3) = \tilde{E}_{z1}(\alpha_n, h_2 + h_3) = \tilde{E}_z(\alpha_n) \quad (54)$$

$$\tilde{H}_{x2}(\alpha_n, h_2 + h_3) - \tilde{H}_{x1}(\alpha_n, h_2 + h_3) = \tilde{J}_z(\alpha_n) \quad (55)$$

$$\tilde{H}_{z2}(\alpha_n, h_2 + h_3) - \tilde{H}_{z1}(\alpha_n, h_2 + h_3) = -\tilde{J}_x(\alpha_n) \quad (56)$$

$$\tilde{E}_{x3}(\alpha_n, 0) = \tilde{E}_{x1}(\alpha_n, 0) = \tilde{E}_{z3}(\alpha_n, 0) = \tilde{E}_{z1}(\alpha_n, 0) = 0 \quad (57)$$

$$\tilde{E}_{x3}(\alpha_n, b) = \tilde{E}_{x1}(\alpha_n, b) = \tilde{E}_{z3}(\alpha_n, b) = \tilde{E}_{z1}(\alpha_n, b) = 0 \quad (58)$$

The fields in each region i are given in terms of the potential functions as

$$E_{zi}(x, y, z) = j\frac{k_i^2 - \beta^2}{\beta}\psi_{ei}(x, y)e^{-j\beta z} \quad (59)$$

$$H_{zi}(x, y, z) = j\frac{k_i^2 - \beta^2}{\beta}\psi_{hi}(x, y)e^{-j\beta z} \quad (60)$$

$$E_{ti}(x, y, z) = \left(\nabla_t\psi_{ei}(x, y) - \frac{\omega\mu_i}{\beta}\hat{z} \times \nabla_t\psi_{hi}(x, y)\right)e^{-j\beta z} \quad (61)$$

$$H_{ti}(x, y, z) = \left(\nabla_t\psi_{hi}(x, y) + \frac{\omega\epsilon_i}{\beta}\hat{z} \times \nabla_t\psi_{ei}(x, y)\right)e^{-j\beta z} \quad (62)$$

where the subscript t indicates the transverse (x or y) component, and

$$\nabla_t = \frac{\partial}{\partial x}\hat{\boldsymbol{x}} + \frac{\partial}{\partial y}\hat{\boldsymbol{y}} \quad (63)$$

In the spectral domain, they are

$$\tilde{E}_{xi}(\alpha_n, y) = -j\alpha_n\tilde{\psi}_{ei}(\alpha_n, y) + \frac{\omega\mu_i}{\beta}\frac{\partial\tilde{\psi}_{hi}(\alpha_n, y)}{\partial y} \quad (64)$$

$$\tilde{E}_{yi}(\alpha_n, y) = j\frac{\alpha_n\omega\mu_i}{\beta}\tilde{\psi}_{hi}(\alpha_n, y) + \frac{\partial\tilde{\psi}_{ei}(\alpha_n, y)}{\partial y} \quad (65)$$

$$\tilde{E}_{zi}(\alpha_n, y) = j\frac{k_i^2 - \beta^2}{\beta}\tilde{\psi}_{ei}(\alpha_n, y) \quad (66)$$

$$\tilde{H}_{xi}(\alpha_n, y) = -j\alpha_n\tilde{\psi}_{hi}(\alpha_n, y) + \frac{\omega\epsilon_i}{\beta}\frac{\partial\tilde{\psi}_{ei}(\alpha_n, y)}{\partial y} \quad (67)$$

$$\tilde{H}_{yi}(\alpha_n, y) = -j\frac{\alpha_n\omega\epsilon_i}{\beta}\tilde{\psi}_{ei}(\alpha_n, y) + \frac{\partial\tilde{\psi}_{hi}(\alpha_n, y)}{\partial y} \quad (68)$$

$$\tilde{H}_{zi}(\alpha_n, y) = j\frac{k_i^2 - \beta^2}{\beta}\tilde{\psi}_{hi}(\alpha_n, y) \quad (69)$$

The solutions of Eq. (38) that satisfy Eqs. (57) and (58) are

$$\tilde{\psi}_{e1}(\alpha_n, y) = A_e \sinh \gamma_1(b - y) \quad (70)$$

$$\tilde{\psi}_{h1}(\alpha_n, y) = A_h \cosh \gamma_1(b - y) \quad (71)$$

$$\tilde{\psi}_{e2}(\alpha_n, y) = B_e \sinh \gamma_2(y - h_3) + C_e \cosh \gamma_2(y - h_3) \quad (72)$$

$$\tilde{\psi}_{h2}(\alpha_n, y) = B_h \sinh \gamma_2(y - h_3) + C_h \cosh \gamma_2(y - h_3) \quad (73)$$

$$\tilde{\psi}_{e3}(\alpha_n, y) = D_e \sinh \gamma_3 y \quad (74)$$

$$\tilde{\psi}_{h3}(\alpha_n, y) = D_h \cosh \gamma_3 y \quad (75)$$

where $A_{e,h}$, $B_{e,h}$, $C_{e,h}$, and $D_{e,h}$ are unknown constants. The fields in the three regions in the spectral domain can now be derived by substituting Eqs. (70) to (75) into Eqs. (64) to (69) as

$$\tilde{E}_{x1}(\alpha_n, y) = -j\alpha_n A_e \sinh \gamma_1(b - y) - \frac{\omega\mu_1\gamma_1}{\beta}A_h \sinh \gamma_1(b - y) \quad (76)$$

$$\tilde{E}_{x2}(\alpha_n, y) = -j\alpha_n[B_e \sinh \gamma_2(y - h_3) + C_e \cosh \gamma_2(y - h_3)] + \frac{\omega\mu_2\gamma_2}{\beta}[B_h \cosh \gamma_2(y - h_3) + C_h \sinh \gamma_2(y - h_3)] \quad (77)$$

$$\tilde{E}_{x3}(\alpha_n, y) = -j\alpha_n D_e \sinh \gamma_3 y + \frac{\omega\mu_3\gamma_3}{\beta}D_h \sinh \gamma_3 y \quad (78)$$

$$\tilde{E}_{z1}(\alpha_n, y) = jA_e\frac{k_1^2 - \beta^2}{\beta} \sinh \gamma_1(b - y) \quad (79)$$

$$\tilde{E}_{z2}(\alpha_n, y) = j\frac{k_2^2 - \beta^2}{\beta}[B_e \sinh \gamma_2(y - h_3) + C_e \cosh \gamma_2(y - h_3)] \quad (80)$$

$$\tilde{E}_{z3}(\alpha_n, y) = jD_e\frac{k_3^2 - \beta^2}{\beta} \sinh \gamma_3 y \quad (81)$$

$$\tilde{H}_{x1}(\alpha_n, y) = -j\alpha_n A_h \cosh \gamma_1(b - y) + \frac{\omega\epsilon_1\gamma_1}{\beta}A_e \cosh \gamma_1(b - y) \quad (82)$$

$$\tilde{H}_{x2}(\alpha_n, y) = -j\alpha_n[B_h \sinh \gamma_2(y - h_3) + C_h \cosh \gamma_2(y - h_3)] - \frac{\omega\epsilon_2\gamma_2}{\beta}[B_e \cosh \gamma_2(y - h_3) + C_e \sinh \gamma_2(y - h_3)] \quad (83)$$

$$\tilde{H}_{x3}(\alpha_n, y) = -j\alpha_n D_h \cosh \gamma_3 y - \frac{\omega\epsilon_3\gamma_3}{\beta}D_e \cosh \gamma_3 y \quad (84)$$

$$\tilde{H}_{z1}(\alpha_n, y) = jA_h\frac{k_1^2 - \beta^2}{\beta} \cosh \gamma_1(b - y) \quad (85)$$

$$\tilde{H}_{x2}(\alpha_n, y) = j\frac{k_2^2 - \beta^2}{\beta}[B_h \sinh \gamma_2(y - h_3) + C_h \cosh \gamma_2(y - h_3)] \quad (86)$$

$$\tilde{H}_{z3}(\alpha_n, y) = jD_h\frac{k_3^2 - \beta^2}{\beta} \cosh \gamma_3 y \quad (87)$$

Applying the boundary conditions Eqs. (49) to (56) using Eqs. (76) to (87) yields

$$\tilde{G}_{11}(\alpha_n, \beta)\tilde{E}_x(\alpha_n) + \tilde{G}_{12}(\alpha_n, \beta)\tilde{E}_z(\alpha_n) = \tilde{J}_x(\alpha_n) \quad (88)$$

$$\tilde{G}_{21}(\alpha_n, \beta)\tilde{E}_x(\alpha_n) + \tilde{G}_{22}(\alpha_n, \beta)\tilde{E}_z(\alpha_n) = \tilde{J}_z(\alpha_n) \quad (89)$$

where $\tilde{G}_{ij}(\alpha_n, \beta)$, $i, j = 1, 2$, are the Green's functions in the spectral domain and can be obtained easily by the spectral-domain immitance approach (9). Using Galerkin's technique, we now express the slots' electric fields as truncated summations of basis functions in the spectral domain as

$$\tilde{E}_x(\alpha_n) \approx \sum_{m=0}^{M} c_m\tilde{E}_{xm}(\alpha_n) \quad (90)$$

$$\tilde{E}_z(\alpha_n) \approx \sum_{k=1}^{K} d_k\tilde{E}_{zk}(\alpha_n) \quad (91)$$

where c_m and d_k are the unknown coefficients, and the basis functions $\tilde{E}_{xm}(\alpha_n)$ and $\tilde{E}_{zk}(\alpha_n)$ describe the x and z electric field distributions on the slots in the spectral domain. Substituting Eqs. (90) and (91) into Eqs. (88) and (89) and taking the inner product of the resultant equations with $\tilde{E}_{xi}(\alpha_n)$, $i = 0, 1, \ldots, M$, and $\tilde{E}_{zj}(\alpha_n)$, $j = 0, 1, \ldots, K$, respectively, results in the following system of coupled linear algebraic equations:

$$\sum_{m=0}^{M} P_{11}^{im}(\beta)c_m + \sum_{k=1}^{K} P_{12}^{ik}(\beta)d_k = 0, \qquad i = 0, 1, 2, \ldots, M \quad (92)$$

$$\sum_{m=0}^{M} P_{21}^{jm}(\beta)c_m + \sum_{k=1}^{K} P_{22}^{jk}(\beta)d_k = 0, \qquad j = 0, 1, 2, \ldots, K \quad (93)$$

where

$$P_{11}^{im} = \sum_{n=1}^{\infty} \tilde{E}_{xi}(\alpha_n)\tilde{G}_{11}(\alpha_n,\ \beta)\tilde{E}_{xm}(\alpha_n) \tag{94}$$

$$P_{12}^{ik} = \sum_{n=1}^{\infty} \tilde{E}_{xi}(\alpha_n)\tilde{G}_{12}(\alpha_n,\ \beta)\tilde{E}_{zk}(\alpha_n) \tag{95}$$

$$P_{21}^{jm} = \sum_{n=1}^{\infty} \tilde{E}_{zj}(\alpha_n)\tilde{G}_{21}(\alpha_n,\ \beta)\tilde{E}_{xm}(\alpha_n) \tag{96}$$

$$P_{22}^{jk} = \sum_{n=1}^{\infty} \tilde{E}_{zj}(\alpha_n)\tilde{G}_{22}(\alpha_n,\ \beta)\tilde{E}_{zk}(\alpha_n) \tag{97}$$

The unknown current densities $\tilde{J}_{x,z}(\alpha_n)$ are eliminated through the use of Parseval's theorem.

The propagation constant β can now be evaluated by setting the determinant of the coefficient matrix of Eqs. (92) and (93) equal to zero and solving for β. The effective dielectric constant is obtained as $\epsilon_{\mathrm{r\,eff}} = (\beta/k_0)^2$, where $k_0 = \omega\sqrt{\epsilon_0\mu_0}$. To obtain numerical results for β, suitable basis functions for the electric field components are needed. These functions should satisfy the same criteria for basis functions discussed in connection with the quasistatic SDA. Here, we employ the following basis functions (10):

$$E_{xm}(x) = \begin{cases} \dfrac{\cos\left(m\pi \dfrac{x-G-S/2}{S}\right)}{\sqrt{1-[2(x-G-S/2)/S]^2}} - \dfrac{\cos\left(m\pi \dfrac{x-G-W-3S/2}{S}\right)}{\sqrt{1-[2(x-G-W-3S/2)/S]^2}}, & m = 0,\ 2,\ \ldots \\ \dfrac{\sin\left(m\pi \dfrac{x-G-S/2}{S}\right)}{\sqrt{1-[2(x-G-S/2)/S]^2}} + \dfrac{\sin\left(m\pi \dfrac{x-G-W-3S/2}{S}\right)}{\sqrt{1-[2(x-G-W-3S/2)/S]^2}}, & m = 1,\ 3,\ \ldots \end{cases} \tag{98}$$

$$E_{zk}(x) = \begin{cases} \dfrac{\cos\left(k\pi \dfrac{x-G-S/2}{S}\right)}{\sqrt{1-[2(x-G-S/2)/S]^2}} - \dfrac{\cos\left(k\pi \dfrac{x-G-W-3S/2}{S}\right)}{\sqrt{1-[2(x-G-W-3S/2)/S]^2}}, & k = 1,\ 3,\ \ldots \\ \dfrac{\sin\left(k\pi \dfrac{x-G-S/2}{S}\right)}{\sqrt{1-[2(x-G-S/2)/S]^2}} + \dfrac{\sin\left(k\pi \dfrac{x-G-W-3S/2}{S}\right)}{\sqrt{1-[2(x-G-W-3S/2)/S]^2}}, & k = 2,\ 4,\ \ldots \end{cases} \tag{99}$$

which are defined only over the slots. Their Fourier transforms are found to be

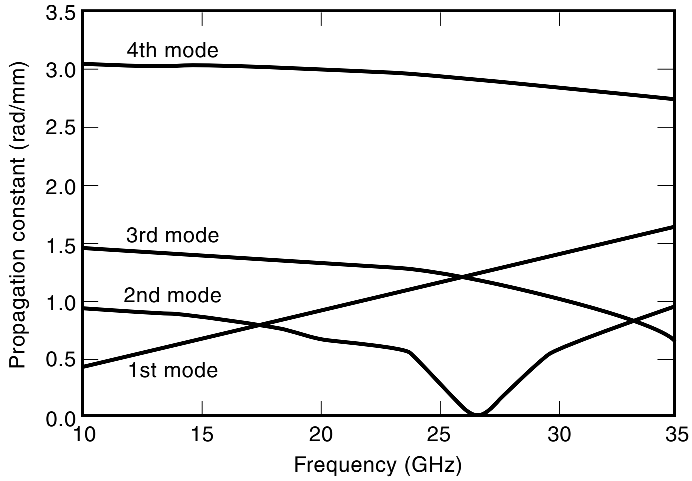

Figure 3. Propagation constants of the first four modes for the coplanar waveguide calculated using the dynamic SDA. a = 60 mil, h_1 = 30 mil, h_2 = 10 mil, h_3 = 20 mil, W = 19.7 mil, $S_1 = S_2 = S$ = 23.6 mil, $\epsilon_{r1} = 1$, $\epsilon_{r2} = 9.6$, $\epsilon_{r3} = 13$.

$$\tilde{E}_{xm}(\alpha_n) = \begin{cases} \dfrac{\pi S}{4}\cos[\alpha_n(G+S/2)]\left[J_0\left(\left|\dfrac{\alpha_n S + m\pi}{2}\right|\right) + J_0\left(\left|\dfrac{\alpha_n S - m\pi}{2}\right|\right)\right] \\ \quad -\dfrac{\pi S}{4}\cos[\alpha_n(G+W+3S/2)]\left[J_0\left(\left|\dfrac{\alpha_n S + m\pi}{2}\right|\right) + J_0\left(\left|\dfrac{\alpha_n S - m\pi}{2}\right|\right)\right], & m = 0, 2, \ldots \\ \dfrac{\pi S}{4}\sin[\alpha_n(G+S/2)]\left[J_0\left(\left|\dfrac{\alpha_n S + m\pi}{2}\right|\right) - J_0\left(\left|\dfrac{\alpha_n S - m\pi}{2}\right|\right)\right] \\ \quad +\dfrac{\pi S}{4}\sin[\alpha_n(G+W+3S/2)]\left[J_0\left(\left|\dfrac{\alpha_n S + m\pi}{2}\right|\right) - J_0\left(\left|\dfrac{\alpha_n S - m\pi}{2}\right|\right)\right], & m = 1, 3, \ldots \end{cases} \tag{100}$$

$$\tilde{E}_{zk}(\alpha_n) = \begin{cases} j\dfrac{\pi S}{4}\sin[\alpha_n(G+S/2)]\left[J_0\left(\left|\dfrac{\alpha_n S + m\pi}{2}\right|\right) + J_0\left(\left|\dfrac{\alpha_n S - m\pi}{2}\right|\right)\right] \\ \quad +\dfrac{\pi S}{4}\sin[\alpha_n(G+W+3S/2)]\left[J_0\left(\left|\dfrac{\alpha_n S + m\pi}{2}\right|\right) + J_0\left(\left|\dfrac{\alpha_n S - m\pi}{2}\right|\right)\right], & k = 1, 3, \ldots \\ \dfrac{\pi S}{4}\cos[\alpha_n(G+S/2)]\left[J_0\left(\left|\dfrac{\alpha_n S + m\pi}{2}\right|\right) - J_0\left(\left|\dfrac{\alpha_n S - m\pi}{2}\right|\right)\right] \\ \quad -\dfrac{\pi S}{4}\cos[\alpha_n(G+W+3S/2)]\left[J_0\left(\left|\dfrac{\alpha_n S + m\pi}{2}\right|\right) - J_0\left(\left|\dfrac{\alpha_n S - m\pi}{2}\right|\right)\right], & k = 2, 4, \ldots \end{cases} \tag{101}$$

An example of computed results from the dynamic SDA is shown in Fig. 3, in which the propagation constants of the first four modes for a CPW are plotted against frequency. The first mode, which is the dominant mode, is found to be propagating up to about 26.5 GHz.

SUMMARY AND CONCLUSIONS

A detailed formulation of the SDA for planar transmission lines has been presented. The SDA obtains the solution of the integral equation method by applying Galerkin's technique in the Fourier transform or spectral domain with high efficiency. SDA is simpler and numerically more efficient than the conventional integral equation method, from which SDA was derived. It has been used extensively for various microwave problems such as planar transmission lines, resonators, antennas, and scattering. The quasistatic SDA produces accurate results only at low frequencies, whereas the dynamic process results in accurate calculations at both low and high frequencies. Because of SDA's attractive features, it has become one of the most popular numerical methods for analyzing microwave and millimeter-wave passive structures, and is expected to remain so.

BIBLIOGRAPHY

1. T. Itoh and R. Mittra, Spectral-domain approach for calculating the dispersion characteristic of microstrip line, *IEEE Trans. Microw. Theory Tech.,* **MTT-21** (7): 498–499, 1973.
2. T. Itoh and A. S. Hebert, A generalized spectral domain analysis for coupled suspended microstriplines with tuning septums, *IEEE Trans. Microw. Theory Tech.,* **MTT-26** (10): 820–826, 1978.
3. D. Mirshekar-Syahkal, *Spectral Domain Method for Microwave Integrated Circuits,* Somerset, UK: Research Studies Press, 1990.
4. T. Itoh, Analysis of microstrip resonators, *IEEE Trans. Microw. Theory Tech.,* **MTT-22** (11): 946–952, 1974.
5. Q. Zhang and T. Itoh, Spectral-domain analysis of scattering from E-plane circuit elements, *IEEE Trans. Microw. Theory Tech.,* **MTT-35** (2): 138–150, 1987.
6. C. Scott, *The Spectral Domain Method in Electromagnetics,* Norwood, MA: Artech House, 1989.
7. T. Kitazawa and T. Itoh, Asymmetrical coplanar waveguide with finite metallization thickness containing anisotropic media, *IEEE MTT-S Int. Microwave Symp. Dig.,* 1990, pp. 673–676.
8. K. M. Rahman and C. Nguyen, On the computation of complex modes in lossless shielded asymmetric coplanar waveguides, *IEEE Trans. Microw. Theory Tech.,* **MTT-43** (12): 2713–2716, 1995.
9. T. Itoh, Spectral-domain immittance approach for dispersion characteristic of generalized printed transmission lines, *IEEE Trans. Microw. Theory Tech.,* **MTT-28** (7): 733–736, 1980.
10. T. Uwano and T. Itoh, Spectral-domain approach, in T. Itoh (ed.), *Numerical Techniques for Microwave and Millimeter-Wave Structures,* Wiley, New York, 1989, pp. 334–380.

CAM NGUYEN
Texas A&M University

SPECTROMETER. See MASS SPECTROMETERS; PARTICLE SPECTROMETERS.

SPECTROMICROSCOPY. See X-RAY MICROSCOPY.

SPECTROSCOPY. See PULSE HEIGHT ANALYZERS.

SPECTROSCOPY, DEEP LEVEL TRANSIENT. See DEEP LEVEL TRANSIENT SPECTROSCOPY.

SPECTROSCOPY, NONLINEAR. See NONLINEAR OPTICS.

SPECTROSCOPY, PHOTOEMISSION. See PHOTOEMISSION.

SPECTRUM EFFICIENCY. See CHANNEL CAPACITY.